

利用适用于SAPO-34的 有机结构导向剂合成SSZ-13分子筛

王磊^{1,2}, 孙毯毯^{2,3}, 闫娜娜², 马超^{2,3,4}, 刘晓娜^{2,3},
田鹏², 郭鹏², 刘中民^{2,3}

(1. 郑州大学化学学院, 绿色催化研究中心, 郑州 450001;
2. 中国科学院大连化学物理研究所甲醇制烯烃国家工程实验室, 洁净能源国家实验室, 大连 116023;
3. 中国科学院大学, 北京 100049; 4. 大连理工大学张煜学院, 大连 116023)

摘要 硅铝分子筛SSZ-13和硅磷铝分子筛SAPO-34已广泛应用于已商业化的催化应用中, 如甲醇制烯烃反应(MTO)和氨气选择性催化还原反应(NH₃-SCR). 目前, 已有多种商业化的有机结构导向剂(OSDA)可用于制备SAPO-34, 而用于合成SSZ-13的OSDA仍主要依赖经典的*N,N,N*-三甲基-1-金刚烷基氢氧化铵(TMAdOH). 因此, 寻找具有较高性价比且可导向合成高硅铝比(SAR)SSZ-13的OSDAs具有重要意义. 本文使用3种可制备SAPO-34的OSDAs[二异丙胺(DIPA)、二丙胺(DPA)、正丁胺(*n*BA)]替代部分TMAdOH, 发现即使不加入晶种也可合成出SSZ-13. 采用粉末X射线衍射(PXRD)和固体核磁共振(ss-NMR)分析方法对制备的SSZ-13进行了系统研究. 结果显示, 所合成的具有可调变SARs的SSZ-13负载Cu之后, 在NH₃-SCR性能上与商业化催化剂相当. 此外, 通过研究DIPA和TMAdOH合成SSZ-13的晶化机理发现, DIPA的加入可以加快结晶过程、提高产率并防止非晶相的形成. 本文提出的观点可为寻找更高效和商业化的SSZ-13结构导向剂及合成具有特定性质的SSZ-13提供参考.

关键词 多孔材料; 分子筛; 结构导向剂; SSZ-13; SAPO-34

中图分类号 O611

文献标志码 A

Exploring Organic Structure-directing Agents Used for SAPO-34 to Synthesize SSZ-13

WANG Lei^{1,2}, SUN Tantan^{2,3}, YAN Nana², MA Chao^{2,3,4}, LIU Xiaona^{2,3},
TIAN Peng², GUO Peng^{2*}, LIU Zhongmin^{2,3}

(1. Green Catalysis Center, College of Chemistry, Zhengzhou University, Zhengzhou 450001, China;
2. National Engineering Laboratory for Methanol to Olefins, Dalian National Laboratory for Clean Energy,
Dalian Institute of Chemical Physics, Chinese Academy of Sciences, Dalian 116023, China;
3. University of Chinese Academy of Sciences, Beijing 100049, China;
4. Zhang Dayu School of Chemistry, Dalian University of Technology, Dalian 116023, China)

Abstract The aluminosilicate zeolite SSZ-13 and zeolitic silicoaluminophosphate molecular sieve (SAPO MS) SAPO-34 have been widely used in commercialized catalytic applications, such as the methanol-to-olefins (MTO) process and the selective catalytic reduction of NO_x with NH₃ (NH₃-SCR). Nowadays, a variety of

收稿日期: 2020-12-09. 网络出版日期: 2021-03-25.

基金项目: 国家自然科学基金(批准号: 21972136, 21676262, 21991091)、中国科学院百人计划(批准号: Y706071202)、中国科学院洁净能源创新研究院合作基金(批准号: DNL201908)和中国科学院前沿科学重点研究计划(批准号: QYZDBSSW-JSC040)资助.

联系人简介: 郭鹏, 男, 博士, 项目研究员, 主要从事分子筛结构解析和表征研究. E-mail: pguo@dicp.ac.cn.

commercialized organic structure-directing agents (OSDAs) have been utilized for preparing SAPO-34, while the OSDAs for synthesizing SSZ-13 still mainly relies on the classical N, N, N -trimethyladamantammonium hydroxide (TMAdaOH). Therefore, it is of great significance to seek for the suitable OSDAs, which can direct the synthesis of SSZ-13 with higher cost performance and applicable high silicon-to-alumina ratio (SAR). Herein, three OSDAs used for preparing SAPO-34 [diisopropylamine (DIPA), dipropylamine (DPA) and n -butylamine (n BA)] were successfully employed for synthesizing SSZ-13 by partial replacing the expensive TMAdaOH with or without the assistance of seeds. Systemic investigation focused on SSZ-13 preparation was explored by powder X-ray diffraction (PXRD) and solid-state nuclear magnetic resonance (ss-NMR) analyses. As a result, the as-synthesized SSZ-13 zeolites possess a tunable range of SARs (11–22) and Cu-SSZ-13 catalysts show excellent NH_3 -SCR performance compared with commercialized ones. The crystallization mechanism of SSZ-13 synthesized by DIPA and TMAdaOH were also studied and the addition of DIPA would accelerate the crystallization process, improve the yields, and prevent the formation of amorphous phase. The work presented here might provide new insights for identifying more efficient and commercialized OSDAs for preparing SSZ-13 with tailored properties.

Keywords Porous material; Zeolite; Organic structure-directing agent; SSZ-13; SAPO-34

1 Introduction

The aluminosilicate zeolite SSZ-13 and zeolitic silicoaluminophosphate molecular sieve (SAPO MS) SAPO-34 with the identical CHA topology have been regarded as the important solid-acid catalysts^[1], especially for the selective catalytic reduction (SCR) of diesel exhaust^[2,3] and the methanol to olefins (MTO) reaction^[4,5]. Therefore, preparations of both catalysts are widely and systematically investigated. Both SSZ-13 and SAPO-34 are three-dimensional (3D) CHA framework containing *cha* cages with small pore openings (delimited by eight tetrahedral atoms such as Si, P, or Al). It is of interest to note that SAPO-34 could be synthesized with tunable Si contents with the assistance of multifarious and economical organic structure-directing agents (OSDAs)^[6–10], while appropriate OSDAs for preparing SSZ-13 are relatively limited. The initial OSDA for synthesizing SSZ-13 was N, N, N -trimethyladamantammonium hydroxide (TMAdaOH)^[11], which has displayed a strong directing capability even in different synthetic systems, such as the traditional hydrothermal method^[12], inter-zeolite transformation^[13], dry gel conversion^[14], and steam-assisted conversion^[15]. However, the utilization of TMAdaOH will come with huge budgets and further impede large-scale industrial production. In this case, developing cost-effective and capable OSDAs to completely or partially replace TMAdaOH has a great practical significance.

A series of quaternary amines imitating the shape of TMAda⁺ cation has been identified for completely replacing TMAda⁺ to synthesize SSZ-13. For example, Itakura *et al.*^[16] used benzyltrimethylammonium hydroxide (BTMOH) as OSDA to synthesize SSZ-13, which would take a longer crystallization time (21 d). Other OSDAs with a similar structural feature were also discovered, namely N, N, N -dimethylethylcyclohexylammonium hydroxide (DMECHAOH) and its bromide^[17,18], but they are not commercially available and require additional chemical preparation. Based on this, a commercialized and security quaternary amine, choline chloride (CC), was selected and could largely reduce the cost^[19,20]. However, it is still challenging to synthesize SSZ-13 with high silicon-to-alumina ratio (SAR) by utilizing CC as the OSDA. Except for the use of traditional organic amines, Ren *et al.*^[21] developed the one-pot method to directly synthesize Cu-SSZ-13 by employing a metal complex Cu-tetraethylenepentamine (Cu-TEPA). This strategy can also relieve the economic burden but is difficult to acquire Cu-free SSZ-13 or SSZ-13 zeolites with tunable SARs. Moreover, it is worth

mentioning that the OSDA-free method, which totally abandons the use of OSDAs, could also be an alternative approach for the preparation of SSZ-13^[22,23]. However, the products still held the low SAR under the hydrothermal condition.

Another route for preparing SSZ-13 is to partially replace TMAdaOH by other OSDAs with a reasonable price. For instance, Martínez-Franco *et al.*^[24] found that the employment of Cu-TEPA and TMAdaOH enabled the synthesis of Cu-SSZ-13 catalysts with controlled SARs and the samples obtained by this modified one-pot method showed good NH₃-SCR performance. Moreover, Guo *et al.*^[25] also developed an economic approach to synthesize SSZ-13 (SAR~10) by using tetramethylammonium hydroxide (TMAOH) and TMAdaOH. The addition of TMAOH not only decreased the consumption of TMAdaOH, but also facilitated crystal growth by bridging the neighboring grains. This signifies that OSDAs appropriate for other zeolites might be favorable to the synthesis of SSZ-13.

Since SAPO-34 and SSZ-13 are closely related from the structural point of view, it would be interesting to attempt to fully or partially utilize commercialized OSDAs used for SAPO-34 to synthesize SSZ-13. However, there are few literatures regarding the direct synthesis of SSZ-13 by using OSDAs of SAPO-34^[26].

Herein, we proposed an economic method to synthesize SSZ-13 through the partial replacement of TMAda⁺ by OSDAs directing the synthesis of SAPO-34. The as-made SSZ-13 samples showed an applicable SAR region (11—22) and the Cu²⁺ exchanged SSZ-13 displayed excellent NH₃-SCR performance.

2 Experimental

The synthesis of SSZ-13 was carried out by the traditional hydrothermal method and the results are listed in Table 1. The detailed synthesis process, catalytic performance tests, and characterization conditions are exhibited in the Supporting Information of this paper.

Table 1 Synthesis of SSZ-13 under different conditions*

Sample	OSDA/Si	TMAda ⁺ /Si	Si/Al	Seeds/SiO ₂	Yield	Product
1	0	0.2	40	10%	74.3%	CHA
2	0.4	0	40	20%	—	No production
3	0.2	0	40	20%	—	No production
4	0.15	0.05	40	10%	73.5%	CHA + MOR + Cri
5	0.15	0.05	27	10%	74.4%	CHA + MOR + Cri
6	0.15	0.05	20	10%	85.1%	CHA + MOR + Cri
7	0.1	0.1	40	10%	69.4%	CHA
8	0.1	0.1	27	10%	76.6%	CHA
9	0.1	0.1	20	10%	80.2%	CHA
10	0.1	0.1	20	0	83.1%	CHA
11	0	0.1	20	0	67.4%	CHA + AP
12	0.1	0.1	40	10%	73.6%	CHA
13	0.1	0.1	40	10%	77.5%	CHA

* The OSDA used for Sample 1 to Sample 10 is DIPA, while OSDAs for Sample 12 and Sample 13 are DPA and *n*BA, respectively; the OSDA/Si, TMAda⁺/Si and Si/Al ratios are calculated in molar ratios while the seeds/SiO₂ ratio is mass ratio; the yield is calculated by dry weight of products and the initial gel, Cri and AP stand for cristobalite and amorphous phase, respectively.

3 Results and Discussion

In our previous work^[27], we have synthesized SAPO-34 with different Si contents by employing various OSDAs, such as diisopropylamine (DIPA), tetraethylammonium hydroxide (TEAOH), *n*-butylamine (*n*BA), and morpholine (MOR). It is of significance to note that unprotonated DIPA could emerge in the pure-silica *cha* cage of high-silica (22.1% in molar ratio) SAPO-34. This finding inspires us to explore OSDAs used for

SAPO-34 to direct the synthesis of the aluminosilicate SSZ-13, replacing TMAdaOH fully or partially.

As shown in Table 1, a series of OSDAs, such as DIPA, dipropylamine (DPA) and *n*BA, were selected for the preparation of SSZ-13 based on the conventional recipe of Sample 1 in molar ratio 20NaOH:20TMAdaOH:2.5Al(OH)₃:100SiO₂:4400H₂O (if needed, seeds would be introduced into the initial gel composition). The PXRD patterns and SEM images are displayed in Fig.S1 and Fig.S2 (see the Supporting Information of this paper). In order to better illustrate the synthesis procedure in detail, one of the secondary amines, DIPA, was chosen. It is worth pointing out that the attempts (Sample 2 and Sample 3) to prepare SSZ-13 by employing DIPA solely failed as shown in Fig.S1 and Table 1, even though the addition of the DIPA and seeds were doubled. It indicates that the complete replacement of OSDAs by DIPA is not feasible. In this case, the strategy of partial replacement was carried out. Replacing three quarters of TMAda⁺ by DIPA will lead to the generation of SSZ-13 with by-products of MOR-type zeolites and cristobalite (Samples 4–6). Pure SSZ-13 with tunable SAR (Samples 7–9) can be obtained with an equal ratio of TMAdaOH and DIPA in the initial gel as listed in Table 1 and Table 2. More importantly, pure SSZ-13 with SAR of 11 (Sample 10) can be successfully prepared even in the absence of SSZ-13 seeds.

Table 2 Chemical compositions and textural properties of Samples 7–13

Sample	Framework composition ^a	SAR ^b	Na/Al ^c	$S_{\text{micro}}^d / (\text{m}^2 \cdot \text{g}^{-1})$	$V_{\text{micro}}^d / (\text{cm}^3 \cdot \text{g}^{-1})$
7	Si _{34.4} Al _{1.6} O ₇₂	21.3	0.20	540.0	0.27
8	Si _{33.8} Al _{2.2} O ₇₂	15.1	0.22	—	—
9	Si _{33.6} Al _{2.4} O ₇₂	13.6	0.23	—	—
10	Si _{33.0} Al _{3.0} O ₇₂	11.3	0.35	529.4	0.26
12	Si _{34.1} Al _{1.9} O ₇₂	17.6	0.30	538.8	0.26
13	Si _{34.0} Al _{2.0} O ₇₂	17.1	0.32	547.4	0.27

a. The framework compositions and Na contents in unit cells were calculated by XRF; *b.* SAR is the molar ratio of Si to Al; *c.* Na/Al molar ratio; *d.* S_{micro} and V_{micro} were determined by *t*-plot method.

We further probe the crystallization mechanisms of SSZ-13 (Sample 10) co-templated by TMAda⁺ and DIPA. Besides, a control sample denoted as Sample 11 was also synthesized for the better comparison. The only difference of synthetic recipes between Sample 10 and Sample 11 is that the DIPA was not added into the gel composition of the latter one. As shown in Fig.1, at the very beginning (0–24 h), the crystallization of SSZ-13 in both Sample 10 and Sample 11 did not take place. The strong peak at 18.4° is attributed to the undissolved Al sources. The changes of this peak indicate that the Si sources dissolved firstly in this system and then Al sources began to dissolve after 12 h. This process could also be verified by SEM as shown in Fig.S3 (see the Supporting Information of this paper). At the time of 24 h, weak PXRD peaks of SSZ-13 could

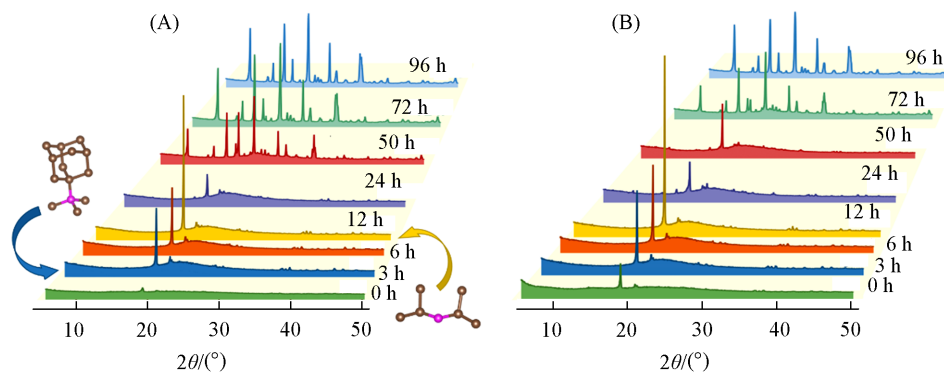


Fig. 1 PXRD patterns of Sample 10(A) and Sample 11(B) during 0–96 h

The insert molecular structures are on behalf of the moment, at which the corresponding organic molecules firstly occurred. The colors of C atoms and N atoms are brown and pink, respectively. H atoms are ignored for clarity.

be detected firstly in both two samples, which means the dissolved Si and Al have formed SSZ-13 (Fig. S3). In addition, the most obvious difference between Sample 10 and Sample 11 is that when the crystallization time arrives at 50 h, the crystallinity of the former one is better, indicating that the introduction of DIPA significantly accelerates the crystallization process (Fig. 1). Moreover, the absence of DIPA will lead to the undesirable amorphous phase (AP) in Sample 11 as displayed in Fig. S2.

For further investigating the incorporation of TMAda^+ and DIPA, ^{13}C MAS NMR characterization of Sample 10 was carried out (Fig. 2). Notably, the chemical shift at δ 22 is attributed to the methyl of DIPA, which can be easily recognized in the whole spectra, while the peak at δ 51 of DIPA is covered by the strong signal of methyl in TMAda^+ at δ 48. Interestingly, the introduction of TMAda^+ firstly occurred at 3 h while DIPA did at 12 h. Besides, it is obvious that although DIPA is present in the as-synthesized SSZ-13, TMAda^+ is still more abundant than DIPA.

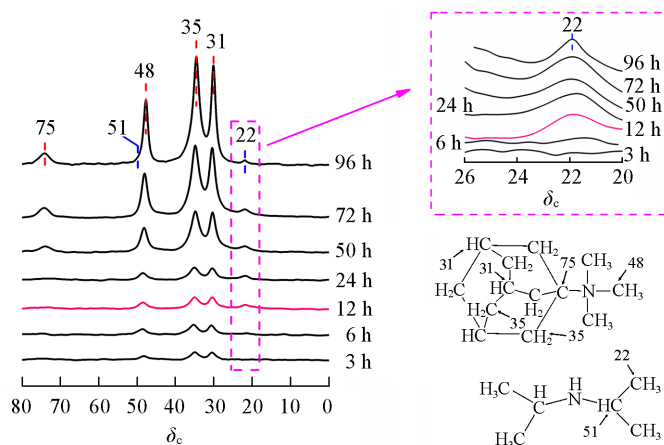


Fig. 2 ^{13}C MAS NMR spectra of Sample 10 at different time

The molecular structures show the chemical shifts affiliations of OSDAs.

In order to investigate the practicability of the as-synthesized SSZ-13 in catalytic fields, Sample 10 was exchanged with $\text{Cu}(\text{OAc})_2$ for NH_3 -SCR tests. For a better comparison, the SSZ-13 seeds used in this work, which were prepared by the classical TMAdaOH , were chosen as a reference for evaluating the catalytic performance. Both SSZ-13 seeds and Sample 10 have a similar SAR of 11 (Table S1, see the Supporting Information of this paper) with an ion-exchange level of *ca.* 60% in terms of the currently commercialized recipe^[28]. As shown in Fig. 3, compared with SSZ-13 seeds, copper exchanged Sample 10 displays no less activity and possesses a wide and applicable active window (200—400 °C) for the diesel vehicle.

In a short summary, by simply replacing part of TMAda^+ by DIPA in the initial gels, SSZ-13 with high crystallinities can be successfully synthesized. The addition of DIPA not only promotes the yield and crystallinity of SSZ-13, but also inhibits the undesirable impure phases. Moreover, the copper exchanged Sample 10 displays excellent NH_3 -SCR performance even after high temperature aging (HTA) at 750 °C for 16 h.

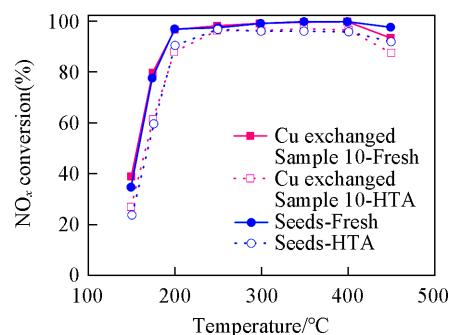


Fig. 3 Results of NH_3 -SCR tests for fresh or HTA Sample 10 and seeds with the same SAR

The reactant feed gas contains 0.05% NO, 0.05% NH_3 , 4.5% H_2O , and 14% O_2 balanced with N_2 . GHSV=300000 h^{-1} with 300 mg of catalysts.

To understand whether effective OSDA replacement is influenced by SAR, three samples with different SARs (denoted as Sample 7, Sample 8, and Sample 9) were selected. The inorganic framework compositions of the three samples were calculated by XRF and are listed in Table 2, while the organic parts were investigated by ^{13}C MAS NMR. The clear trend shown in Fig.4 demonstrates that there are more DIPAs incorporated with the increase of SARs.

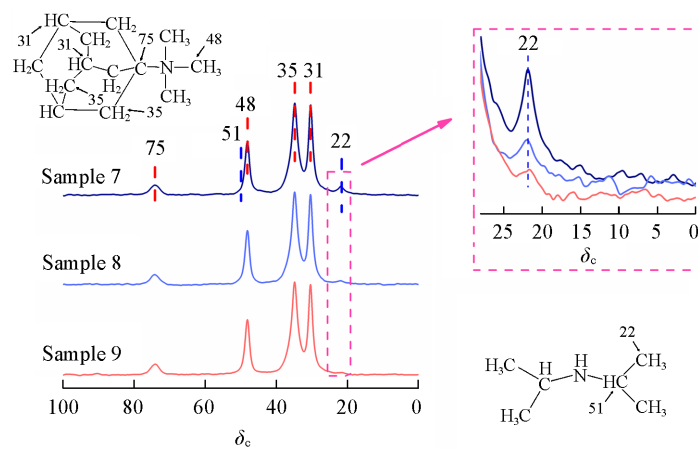


Fig. 4 ^{13}C MAS NMR spectra of SSZ-13 with different SAR

The molecular structures show the chemical shifts affiliations of OSDAs.

Now that the partial replacement of TMAdaOH by DIPA is successful, other frequently-used OSDAs for SAPO-34 might be feasible. To verify this hypothesis, DPA and *n*BA were employed for the partial replacement of TMAdaOH to prepare SSZ-13, and it turns out that well-crystallized SSZ-13 (Sample 12 and Sample 13) can be successfully obtained as shown in Table 1. There is no doubt that DPA and *n*BA have been introduced into SSZ-13 according to the results of ^{13}C MAS NMR spectra (Fig.5). Furthermore, the amounts of *n*BA in the SSZ-13 cages are higher than DIPA as observed in the higher intensity of δ 22 from *n*BA than the one from DIPA (inset of Fig. 5). It is attributed to the fact that there are two *n*BAs locating in one *cha* cage, while only one DIPA occupies one *cha* cage^[29].

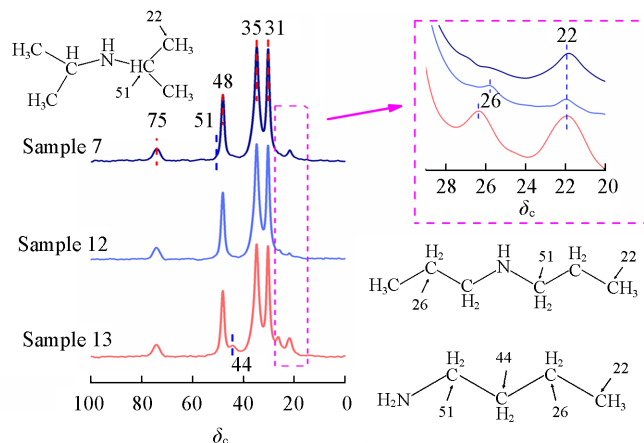


Fig. 5 ^{13}C MAS NMR spectra of SSZ-13 prepared with different OSDAs

The molecular structures show the chemical shifts affiliations of OSDAs.

4 Conclusions

In this work, we have synthesized well-crystallized SSZ-13 by employing TMAdaOH and OSDAs used for SAPO-34 (DIPA, DPA, and *n*BA). The studies on the crystallization mechanisms of SSZ-13 co-templated by

TMAdaOH and DIPA were carried out. The results show that the partial replacement of expensive TMAdaOH by DIPA accelerates the crystallization process, inhibits the formation of amorphous phase, and increases the yields. The Cu-SSZ-13 shows excellent NH₃-SCR reactivity even compared with recent state-of-art catalysts.

The supporting Information of this paper see <http://www.cjcu.jlu.edu.cn/CN/10.7503/cjcu20200855>.

This paper is supported by the National Natural Science Foundation of China (Nos.21972136, 21676262, 21991091), the CAS Pioneer Hundred Talents Program (No.Y706071202), the Dalian National Laboratory for Clean Energy (DNL) Cooperation Fund, Chinese Academy of Sciences (No.DNL201908) and the Key Research Program of Frontier Sciences, Chinese Academy of Sciences (No. QYZDBSSW-JSC040).

References

- [1] Dusselier M., Davis M. E., *Chem. Rev.*, **2018**, *118*(11), 5265—5329
- [2] Beale A. M., Gao F., Lezcano-Gonzalez I., Peden C. H. F., Szanyi J., *Chem. Soc. Rev.*, **2015**, *44*(20), 7371—7405
- [3] Mohan S., Dinesha P., Kumar S., *Chem. Eng. J.*, **2020**, *384*, 123253
- [4] Tian P., Wei Y., Ye M., Liu Z., *ACS Catal.*, **2015**, *5*(3), 1922—1938
- [5] Yang M., Fan D., Wei Y., Tian P., Liu Z., *Adv. Mater.*, **2019**, *31*(50), 1902181
- [6] Marchese L., Frache A., Gianotti E., Martra G., Causà M., Coluccia S., *Microporous Mesoporous Mater.*, **1999**, *30*(1), 145—153
- [7] Qiao Y. Y., Wu P. F., Xiang X., Yang M., Wang Q. Y., Tian P., Liu Z. M., *Chin. J. Catal.*, **2017**, *38*(3), 574—582 (乔昱焱, 吴鹏飞, 向骁, 杨森, 王全义, 田鹏, 刘中民. 催化学报, **2017**, *38*(3), 574—582)
- [8] Fan D., Tian P., Xu S., Wang D., Yang Y., Li J., Wang Q., Yang M., Liu Z., *New J. Chem.*, **2016**, *40*(5), 4236—4244
- [9] Aghamohammadi S., Haghighi M., *Adv. Powder Technol.*, **2016**, *27*(4), 1738—1749
- [10] Sadeghpour P., Haghighi M., *Particuology*, **2015**, *19*, 69—81
- [11] Zones S. I., *Zeolite SSZ-13 and Its Method of Preparation*, US Patent 4544538, 1985—10—01
- [12] Wang Y., Wang C., Wang J., Wang J., Wang L., Xu C., Shen M., *Materials*, **2020**, *13*(8), 1829
- [13] Tang L., Haw K. G., Zhang Y., Fang Q., Qiu S., Valtchev V., *Microporous Mesoporous Mater.*, **2019**, *280*, 306—314
- [14] Al Jabri H., Miyake K., Ono K., Nakai M., Hirota Y., Uchida Y., Miyamoto M., Nishiyama N., *Microporous Mesoporous Mater.*, **2019**, *278*, 322—326
- [15] Zeng L., Yu Z., Sun Z., Han Y., Xu Y., Wu J., Liang Z., Wang Z., *Microporous Mesoporous Mater.*, **2020**, *293*, 109789
- [16] Itakura M., Inoue T., Takahashi A., Fujitani T., Oumi Y., Sano T., *Chem. Lett.*, **2008**, *37*(9), 908—909
- [17] Cao G., Mertens M. M., Guran A. S., Li H., Yoder J. C., *Synthesis of Chabazite-containing Molecular Sieves and Their Use in the Conversion of Oxygenates to Olefins*, US 7754187 B2, 2010—07—13
- [18] Xiong X., Yuan D., Wu Q., Chen F., Meng X., Lv R., Dai D., Maurer S., McGuire R., Feyen M., Müller U., Zhang W., Yokoi T., Bao X., Gies H., Marler B., Vos D. E. D., Kolb U., Moini A., Xiao F., *J. Mater. Chem. A*, **2017**, *5*(19), 9076—9080
- [19] Chen B., Xu R., Zhang R., Liu N., *Environ. Sci. Technol.*, **2014**, *48*(23), 13909—13916
- [20] Xu R., Zhang R., Liu N., Chen B., Qiao S. Z., *ChemCatChem*, **2015**, *7*(23), 3842—3847
- [21] Ren L., Zhu L., Yang C., Chen Y., Sun Q., Zhang H., Li C., Nawaz F., Meng X., Xiao F. S., *Chem. Commun.*, **2011**, *47*(35), 9789—9791
- [22] Imai H., Hayashida N., Yokoi T., Tatsumi T., *Microporous Mesoporous Mater.*, **2014**, *196*, 341—348
- [23] Nasser G. A., Muraza O., Nishitoba T., Malaibari Z., Al-Shammari T. K., Yokoi T., *Microporous Mesoporous Mater.*, **2019**, *274*, 277—285
- [24] Martínez-Franco R., Moliner M., Thøgersen J. R., Corma A., *ChemCatChem*, **2013**, *5*(11), 3316—3323
- [25] Guo Y., Sun T., Liu X., Ke Q., Wei X., Gu Y., Wang S., *Chem. Eng. J.*, **2019**, *358*, 331—339
- [26] Luan H. M., Chen W., Wu Q. M., Xu H., Han S. C., Meng X. J., Zheng A. M., Xiao F. S., *Chem. J. Chinese Universities*, **2020**, *41*(7), 1470—1476 (栾慧敏, 陈伟, 吴勤明, 徐好, 韩世超, 孟祥举, 郑安民, 肖丰收. 高等学校化学学报, **2020**, *41*(7), 1470—1476)
- [27] Wang L., Sun T. T., Yan N. N., Liu X. N., Ma C., Xu S. T., Guo P., Tian P., Liu Z. M., *Acta Phys.-Chem. Sin.*, doi:10.3866/PKU.WHXB202003046 (王磊, 孙毯毯, 闫娜娜, 刘晓娜, 马超, 徐舒涛, 郭鹏, 田鹏, 刘中民. 物理化学学报, doi:10.3866/PKU.WHXB202003046)
- [28] Song J., Wang Y., Walter E. D., Washton N. M., Mei D., Kovarik L., Engelhard M. H., Prodingner S., Wang Y., Peden C. H. F., Gao F., *ACS Catal.*, **2017**, *7*(12), 8214—8227
- [29] Yan N., Xu H., Zhang W., Sun T., Guo P., Tian P., Liu Z., *Microporous Mesoporous Mater.*, **2018**, *264*, 55—59

(Ed.: N, K, M)